Towards a thermodynamical description of dense granular media

Vittorio Loreto
Università degli Studi di Roma "La Sapienza", Dipartimento di Fisica and INFM Unità di Roma 1, P.le A. Moro 5, 00185 Rome, Italy
(May 4, 2001)

In this talk I will discuss whether thermodynamical and in particular entropic concepts could be relevant for the relaxation dynamics in granular systems. Since in these systems energy is lost through internal friction, and gained by a non-thermal source such as tapping or shearing, this approach seems doomed from the outset.
I will focus first on a mean-field model where it is possible to construct explicitly a *free-energy*-like functional which decreases along the trajectories of the dynamics and which allows to account for the asymptotic behavior: e.g. density profile, segregation phenomena.
Furthermore I will consider two classes of finite-dimensional systems which well describe the compaction dynamics of a granular medium and present numerical evidences which support Edwards's hypothesis that macroscopic observables of dense granular media can be evaluated from averages over *typical* blocked configurations. I will show how it is possible, for such a systems, to construct the corresponding measure and compare its predictions for various observables with the outcome of the out of equilibrium dynamics at large times.

I. INTRODUCTION

In this talk I will discuss and report results obtained in the last few years in close collaboration with a few people whom I'm pleased to quote. In particular I have been working on these subjects with Alain Barrat, Emanuele Caglioti, Jorge Kurchan and Mauro Sellitto. All the results I will discuss would simply not be there without their contributions [1–3].

Granular systems [4,5] involve many particles, so there is a strong motivation to treat them with thermodynamic methods. This approach is justified when one is able to identify a distribution that is left invariant by the dynamics (*e.g.* the microcanonical ensemble), and then assume that this distribution will be reached by the system, under suitable conditions of 'ergodicity'. Unfortunately, because energy is lost through internal friction, and gained by a non-thermal source such as tapping or shearing, the dynamical equations do not leave the microcanonical or any other known ensemble invariant. Moreover, just as in the case of aging glasses, the compaction dynamics does not approach any stationary state on experimental time scales and these systems exhibit aging [6,7] and memory [8,9]. This raises several questions and among them the most important is whether it is possible in principle to construct a coherent thermodynamics for these "non-thermal" systems.

Just to fix the ideas and give a concrete example of the typical difficulty one would like to be able to overcome, let us consider a compaction experiment, in which we subject a granular system to gentle, periodic tapping. To keep the discussion simple, we can assume that there is no gravity, and that there is a piston applying a constant pressure on the surface. The system compactifies very slowly [10], in practice never reaching the most dense, optimal packing. At a given long time, when the system has density $\rho(t)$, we may wish to measure for example the fraction of grains that are at relative distance r: the structure factor. This quantity being averaged over all particles, one can expect it to be a reproducible observable. However, there is in principle no method to calculate the structure factor other than solving the dynamics.

Some years ago Edwards [11–14] proposed that one could reproduce the observables attained dynamically by calculating the value they take in the usual equilibrium distribution at the corresponding volume, energy, etc. *but restricting the sum to the 'blocked' configurations* defined as those in which every grain is unable to move [15]. In the case of the previous paragraph, we would compute the structure factor in *all the possible* blocked configurations of density $\rho(t)$, and calculate the average. Thus, the only input from dynamics would be $\rho(t)$, apart from which the calculation is based on a statistical ensemble.

This 'Edwards ensemble' leads immediately to the definition of an entropy (in the glass literature a 'complexity') S_{Edw}, given by the logarithm of the number of blocked configurations of given volume, energy, etc., and its corresponding density $s_{Edw} \equiv S_{Edw}/N$. Associated with this entropy are state variables such as 'compactivity' $X_{Edw}^{-1} = \frac{\partial}{\partial V} S_{Edw}(V)$ and 'temperature' $T_{Edw}^{-1} = \frac{\partial}{\partial E} S_{Edw}(E)$.

The main purpose of this talk is to try to substantiate this hypothesis and to address the natural question of whether Edwards' measure could give good results for the compaction of realistic finite dimensional, non mean-field models.

The talk will be organized along the following lines. We first try to exploit the analogy between the settling of grains and powders, and the aging of glassy systems [17] since in both cases, the system remains out of equilibrium on all accessible time-scales, and displays very slow relaxations. In this spirit we shall discuss in Sect.II which informations one can extract from solvable mean-field models for glasses. Sect.III will be devoted to the discussion of a mean field model explicitly conceived for granular media and where the it is possible to construct explicitly a *free-energy*-like functional which decreases along the trajectories of the dynamics and where the role of the temperature and the interplay between entropic and dynamical effects is particularly evident. Section IV introduces Edwards' hypothesis and in sections V and VI we apply these ideas by treating two finite-dimensional models which reproduce many of the features of glasses and granular media, namely the Kob-Andersen (KA) [18] and Tetris [19] models. We devise a method to count and calculate averages over the blocked configurations, explicitly constructing in this way Edwards' measure. We compare expectation values thus obtained with equilibrium values and with the outcome of slow, aging dynamics and find very good agreement between the predictions of Edwards' measure and aging dynamics. A few remarks will follow and conclude the talk.

II. SOLVABLE GLASSY MODELS

In the late eighties, Kirkpatrick et al. [20,21] recognized that a class of mean-field models contains, although in a rather schematic way, the essentials of glassy phenomena. When the aging dynamics of these systems was solved analytically, a feature that emerged was the existence of a temperature T_{dyn} for *all* the slow modes (corresponding to structural rearrangements) [22,23].

For the purposes of this paper, T_{dyn} can be defined by comparing the random diffusion and the mobility between two widely separated times t and t_w of any particle or tracer in the aging glass. Surprisingly, one finds in all cases an Einstein relation $\left\langle (r(t) - r(t_w))^2 \right\rangle = T_{dyn} \frac{\delta \langle r(t) - r(t_w) \rangle}{\delta f}$, where r is the position of the particle and f is a constant perturbing field, and the brackets denote average over realizations. While in an equilibrium system the fluctuation-dissipation theorem guarantees that the role of T_{dyn} is played by the thermodynamic temperature, the appearance of such a quantity out of equilibrium is by no means obvious. T_{dyn} is different from the external temperature, but it can be shown to have all other properties defining a true temperature [23].

As it turned out, despite its very different origin, this temperature matches exactly Edwards' ideas. One can identify in mean-field models all the energy minima (the blocked configurations in a gradient descent dynamics), and calculate $1/T_{Edw}$ as the derivative of the logarithm of their number with respect to energy. An explicit computation shows that T_{Edw} coincides with T_{dyn} obtained from the out of equilibrium dynamics of the models aging in contact with an almost zero temperature bath [24–29]. Moreover, given the energy $E(t)$ at long times, the value of any other macroscopic observable is also given by the flat average over all blocked configurations of energy $E(t)$. Within the same approximation, one can also treat systems that like granular matter present a non-linear friction and different kinds of energy input, and the conclusions remain the same [30] despite the fact that there is no thermal bath temperature.

Edwards' scenario then happens to be correct within mean-field schemes and for very weak vibration or forcing. The problem that remains is to what extent it carries through to more realistic models.

III. N-PLANES MODEL: A MEAN-FIELD MODEL FOR GRANULAR MEDIA

In this section we consider in detail a mean-field model explicitly conceived for the relaxation dynamics of granular media. This will help us to understand the interplay between entropic and dynamical effects. We consider, in particular, a simple model which describes the evolution of a system of particles which hop on a lattice of $k = 0, ..., N$ stacked planes, as introduced in [19] and discussed in [1]. In particular the system represents an ensemble of particles which can move up or down in a system of N layers in such a way that their total number is conserved. We ignore the correlations among particles rearrangements and problems related to the mechanical stability of the system. The master equation for the density on a generic plane k, except for the $k = 0$ plane, is given by:

$$\begin{aligned}\partial_t \rho_k = (1-\rho_k) D(\rho_k) [\rho_{k-1} \cdot p_{up} + \rho_{k+1} \cdot p_{down})] + \\ -\rho_k [(1-\rho_{k-1}) D(\rho_{k-1}) p_{down} + \\ +(1-\rho_{k+1}) D(\rho_{k+1}) p_{up}] \qquad (1)\end{aligned}$$

where p_{down} and p_{up} (with $p_{up} + p_{down} = 1$) represents the probability for the particles to move downwards or upwards, respectively, among the different planes. With p_{up} and p_{down} we can define the quantity $x = p_{up}/p_{down}$ which quantifies the importance of gravity in the system. We can also associate to x a sort of temperature for the system given by $T \sim 1/log(1/x)$. We shall return to this point later on.

$D(\rho_k)$ represents a sort of mobility for the particles given by the probability that the particle could find enough space to move. Apart from other effects it mainly takes onto account the geometrical effects of frustration, i.e. the fact that the packing prevents the free movement of the particles.

Later on we shall show how the analysis reported here is very general and does not depend on the exact functional form chosen for $D(\rho)$. For the sake of clarity before discussing the problem in its generality we shall consider a possible functional form for $D(\rho_k)$ suitable for the compaction problem. In a naive way one could imagine a functional form like $D(\rho_k) = \rho_k(1-\rho_{k'})$ obtained by considering only the interactions with the nearest neighbors planes whose density is designed by $\rho_{k'}$. It is easy to realize that such an approach does not account for the complexity of the problem where the packing at high densities creates long range correlations in the system, and, using this functional form, the equations show a trivial relaxation. A possible general form of $D(\rho_k)$, which can be seen as the outcome of a theory based on the existence of regions of cooperativity [31] (as well as of a free-volume theory [32,33]) for granular media, includes a term like

$$D(\rho_k) = D_0 \exp[-\alpha/(1-\rho_k)]. \tag{2}$$

The parameter α quantifies how much the shape and the dimensions of the particle frustrate its motion. Higher is α higher will be the geometrical frustration felt by the corresponding particle. For instance in the problems of parking of r-mers (i.e. segments of length r) on a line, under the hypothesis of an exponential distribution for the lengths of the empty (or filled) intervals, the probability for each r-mer to find a sufficient space to land is $\exp(-r/(1-\rho))$, where ρ is the occupation density on the line [32].

The question we want to address is whether there exists a variational principle driving the relaxation phenomena in this system and in general in granular media. In other words one could ask if, in analogy with what happens for a liquid system, there exists some free-energy-like functional minimized (Lyapunov functional) [34] by the dynamical evolution. In a very general way it is possible to write explicitly a Lyapunov functional for the system of equations (1), say the functional which decreases monotonically along the trajectories of the motion. This functional can be cast in the form of a free-energy-like function:

$$F = \sum_{k=0}^{\infty} [\gamma(x) k \rho_k - S(\rho_k)] \tag{3}$$

where the $S(\rho_k)$, the *entropic*-like contribution, and $\gamma(x)$ have to be determined in a self-consistent way by imposing that F decreases for any exchange of particles between two generic planes k and $k+1$. Writing explicitly the expression for dF for a generic particle exchange and imposing $dF \leq 0$, for the particular choice of $D(\rho_k)$ we made, after some manipulations one gets for the functional (3) the expressions

$$S(\rho_k) = \rho_k log(\frac{1-\rho_k}{\rho_k}), \quad \gamma(x) = log(\frac{1}{x}). \tag{4}$$

Let us stress how $S(\rho_k)$ has exactly the same (critical) behavior, as $\rho_k \to 1$, of the entropy of a one-dimensional continuous system, filled with bars of unitary length at a certain density ρ. The functional F is a concave function because $\partial^2 F/\partial \rho_k^2 \geq 0 \ \forall k$ [35].

As a consequence there exists a unique minimum for this functional and this minimum should correspond to the stationary state of the system. In the case of a monodisperse system we expect that the stationary state (i.e. the density profile for the system) is the one obtained, in a continuous process of shaking, after a very long transient.

In the general case with arbitrary N, and for $N \to +\infty$, it is possible to get the exact asymptotic stationary solution for the density on each plane. We denote with M the total "mass" of the system, i.e. the maximal number of planes which can be completely filled. Using a standard Lagrange multiplier method, where one tries to find the extremum of F subject to to the constraint $\sum_k \rho_k = M$, the solution is given by the following implicit expression:

$$f(\rho_k) = f(\rho_0) x^k \tag{5}$$

where

$$f(s) = \frac{s}{1-s} e^{\frac{1}{1-s}}, \tag{6}$$

and ρ_0 is the density on the zero-th plane which is a complex function of the total mass of the system. In order to visualize the solution it is possible to extract the approximate explicit behaviors. In particular one gets:

$$\rho_k^{\infty} \simeq 1 - 1/[(M-k) \cdot \log(1/x)] \text{ for } k << M \tag{7}$$

$$\rho_k^{\infty} \simeq e^{(M-k)\cdot \log(1/x)} \text{ for } k >> M. \tag{8}$$

The stationary solution tends thus to a step function $\theta(k-M)$ in the limit $x \to 0$. This behavior is very well verified in the experiments [36].

Let us now ask what happens considering a bidisperse system, i.e. by considering two kind of particles defined by two different values of α ($\alpha_s = 1, \alpha_b = \alpha = 2$ in the specific case). In the case the master equations for the densities ρ_k^b and ρ_k^s on a generic plane k, except for the plane $k=0$, are given by:

$$\begin{aligned}\partial_t \rho_k^{b,s} &= D^{b,s}(\rho_k)[\rho_{k-1}^{b,s} p_{up} + \rho_{k+1}^{b,s} p_{down})] + \\ &\quad -\rho_k^{b,s}[D^{b,s}(\rho_{k-1}) p_{down} + D^{b,s}(\rho_{k+1}) p_{up}]\end{aligned} \tag{9}$$

where $\rho_k = \rho_k^s + \alpha \rho_k^b$ is the total density on the k-th plane and $D^{b,s}(\rho_k)$ are the probabilities for a particle s or b respectively, landing on the plane k, to fit the local geometrical environment. In this sense $D^{b,s}(\rho)$ are the analog of the mobilities for the two kind of particles and they take into account the cooperative effects on the dynamics generated by the frustration. A possible functional form for $D^{b,s}(\rho)$ (see for a similar approach [32,19,33,31]), is given by $D^s(\rho) \sim (1-\rho)\exp[-1/(1-\rho)]$ and $D^b(\rho) \sim (1-\rho)^{\alpha} \exp[-\alpha/(1-\rho)]$ with $\alpha \geq 1$.

Let us now look for a Lyapunov functional equivalent to Eq.(3) in this polydisperse case which now will have the form:

$$F = \sum_{k=0}^{\infty} [\gamma(x) n \rho_k - S(\rho_k^b, \rho_k^s)] \qquad (10)$$

where the $S(\rho_k^b, \rho_k^s)$ is again an *entropic*-like contribution. By repeating the calculation along the same lines as before one gets

$$S(\rho_k^b, \rho_k^s) = -\rho_k^s (log(\rho_k^s) - 1) - \rho_k^b (log(\rho_k^b) - 1) \\ -(1-\rho_k)(log(1-\rho_k) - 1) + log(1-\rho_k) \quad (11)$$

and $\gamma(x) = log(1/x)$.

Even in this case the functional F is concave and there exists a unique solution corresponding to the asymptotic stationary state for the system. Using a standard Lagrange multiplier method one gets the result:

$$\rho_k^b = \rho_k \frac{h_0 (1-\rho_k)^{\alpha-1} e^{-\frac{\alpha-1}{1-\rho_k}}}{1 + \alpha h_0 (1-\rho_k)^{\alpha-1} e^{-\frac{\alpha-1}{1-\rho_k}}} \\ \rho_k^s = \rho_k - \alpha \rho_k^b \qquad (12)$$

where $h_0 = h_0(\rho_0^b, \rho_0^s)$ is a constant which can be estimated by using the total mass M of the system:

$$h_0(\rho_0^b, \rho_0^s) = (1-\rho_0)^{1-\alpha} e^{\frac{\alpha-1}{1-\rho_0}} \frac{\rho_0^b}{\rho_0^s}. \qquad (13)$$

ρ_k is given by a non trivial function of k that can be obtained exactly but in a implicit form. ρ_k is a monotonically decreasing function with the maximum for $k = 0$. Fig. 1 shows an example of the asymptotic stationary solution obtained from (12) with $h_0 \simeq 10^3$ corresponding to $x \simeq 0.82$, $\rho_0 = 1 - \frac{c}{M log(1/x)} \simeq 0.9$ and $\frac{\rho_0^b}{\rho_0^s} \simeq 1.5 \cdot 10^{-3}$. In particular it shows ρ_k^b and ρ_k^s as a function of ρ_k. In this way the effect of segregation [37] of the "big" particles (with $\alpha = 2$) on top of the "small" ones (with $\alpha = 1$) is clearly visible. The introduction of two different weights for the two species, say $p_{up}^{b,s}$ and $p_{down}^{b,s}$, gives rise to a rich phase space $(p_{up}^b, p_{up}^s, \alpha)$ with different regions corresponding to different behaviors for segregation.

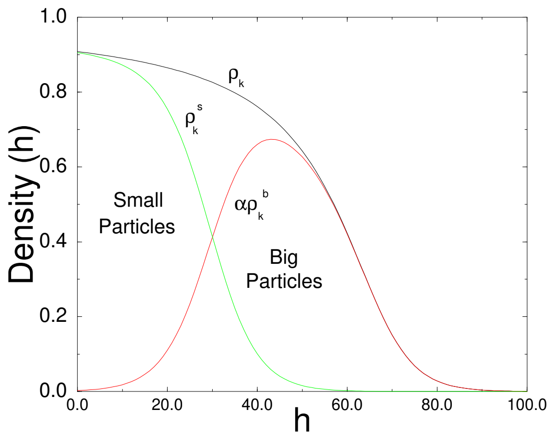

FIG. 1. Asymptotic density profile for the two species of particles in the N-planes model described in the text. It is clearly visible the effect of segregation of the more frustrated (big) particles ρ_b^k on top of the less frustrated (small) ones ρ_b^k.

Eq.(11) makes evident how in the dynamics of granular media entropic effects are far from being negligible and the global behavior is given by a complex interplay between gravitational and entropic-like effects.

Let us now continue to push forward this point of view and ask whether the asymptotic stationary state corresponds to some sort of equilibrium state. At the equilibrium, i.e. asymptotically, one would expect that for any exchange of particles among different planes $dF = 0$ for the free-energy-like functional (10), or equivalently $dS/dE = 1/T = const.$. By defining the total energy $E = \sum_{k=0}^{\infty} k \rho_k$ and the total entropy $S_{tot} = \sum_{k=0}^{\infty} S(\rho_k)$, for any exchange of particles of type b or s between the planes k and $k+1$ one has:

$$\frac{dS_{tot}^{b,s}}{dE} = \frac{\partial S(\rho_{k+1})}{\partial \rho_{k+1}^{b,s}} - \frac{\partial S(\rho_k)}{\partial \rho_k^{b,s}}. \qquad (14)$$

It is easy to realize how in the asymptotic stationary state one has

$$\frac{dS_{tot}^s}{dE} = \frac{dS_{tot}^b}{dE} = log(\frac{1}{x}) = const., \qquad (15)$$

or, what is the same, $\frac{dS_{tot}^{b,s}}{dE} = const.$ everywhere in the system no matter which kind of particles we use for its definition. It is then tempting to associate $log(\frac{1}{x})$ with the inverse of a temperature for the system. The analogy is made stronger by recalling that $1/log(\frac{1}{x})$ is the usual quantity associated to a temperature in Monte-Carlo dynamics. From this point of view the relaxation process of this system would correspond to an equilibration procedure in which $\frac{dS_{tot}^{b,s}}{dE}$ is made uniform everywhere. In the specific case of segregation one is forced to think that the system evolves in such a way that asymptotically all the particles have the same mobility, measured in this case in terms of the entropic change for every given displacement.

Let us now generalize the results obtained so far. Eq.(1) represents a particular case of a general class of equations that can be written as:

$$\partial_t \rho_k = g(\rho_k)[f(\rho_{k-1})p_{up} + f(\rho_{k+1})p_{down})] + \\ -f(\rho_k)[g(\rho_{k-1})p_{down} + g(\rho_{k+1})p_{up}] \qquad (16)$$

where f and g are generic functions for which we only require $f \geq 0$, $g \geq 0$, $df/d\rho \geq 0$, $dg/d\rho \leq 0$. All the results we have shown in the particular case (1) are valid under these general assumptions. In particular we can prove that there does exist a functional that decreases along the trajectories of the motion and its expression is given by Eq.(3) with:

$$S(\rho_k) = \int_{\rho_k} log\frac{g(\rho)}{f(\rho)}d\rho, \qquad \gamma(x) = log(\frac{1}{x}). \qquad (17)$$

A deeper insight in the above mentioned phenomenology is obtained by considering the continuum limit for the model described by Eq.(16). More precisely we consider a diffusive limit that consists in scaling the space variable as $\frac{1}{\epsilon}$, the time variable as $\frac{1}{\epsilon^2}$ and the drift term $p_{down}-p_{up}$ as ϵ. Therefore $x = \epsilon k$, $\tau = \epsilon^2 k/2$, $p_{down} - p_{up} = \epsilon\beta/2$ and we consider the evolution of $u(x) \equiv \rho(k)$.

We get the continuum limit by taking the Taylor expansion of the right member of Eq.(16) around $x = k\epsilon$. For example $\rho(k+1) \equiv u(x+\epsilon) = u(x)+\epsilon\partial_x u+\frac{1}{2}\epsilon^2\partial_{xx}u+O(\epsilon^3)$.

We get, formally,

$$\partial_\tau u(x) = \beta\partial_x(fg) + (g\partial_{xx}f - f\partial_{xx}g) + O(\epsilon), \qquad (18)$$

which, in the limit $\epsilon \to 0$, gives

$$\partial_\tau u(x) = \beta\partial_x(fg) + (g\partial_{xx}f - f\partial_{xx}g). \qquad (19)$$

This is a non linear diffusion equation that may be conveniently written in the following form

$$\partial_\tau u = \partial_x\left(D(u)\partial_x\frac{\partial F}{\partial_u}\right), \qquad (20)$$

where $D = fg$, $\frac{\partial F}{\partial_u}$ denotes the functional derivative of F with respect to u, $F = \int_0^\infty(\beta\ u\ x - S(u))dx$, and $S' = \log\left(\frac{g}{f}\right)$. Notice that the functional F decreases with the dynamics induced by Eq. (19). One has, in fact,

$$\partial_\tau F = \int dx\frac{\partial F}{\partial u}\partial_\tau u = \int dx\frac{\partial F}{\partial u}\partial_x\left(D(u)\partial_x\frac{\partial F}{\partial u}\right) \qquad (21)$$

that, after an integration by parts, gives

$$-D(u)\left(\frac{\partial F}{\partial_u}\right)^2 \leq 0. \qquad (22)$$

Therefore there exists a "free energy"-like functional, F, for Eq. (20) which has exactly the same form of the functional defined for the discrete model (see Eq.(17)). We can notice that while the functional form of S and the value of β determine in a unique way the asymptotic state they are not sufficient to determine the dynamical behavior of the system. In particular in order to know it one should know the functional form of $D(\rho)$.

What we have discussed so far suggests the possibility of introducing, for non-thermal systems as granular media, equilibrium concepts as free-energy, entropy and temperature. More precisely it is possible (in the case studied here) to predict the asymptotic state by means of the minimization of a suitable functional which can be constructed by entropic arguments. It is worth stressing how granular systems often exhibit memory and so the existence of a unique Lyapunov functional is not guaranteed in general. In general one could expect that several Lyapunov functionals are associated to different stationary states reached with different dynamical paths.

Finally let us notice how Eq.(20) allows us to comment on the relationship between entropic and dynamical effects in explaining the relaxation phenomena in granular media. Once the Lyapunov functional is known (and thus also the entropic properties of the system) it is possible to predict the asymptotic state. However one cannot specify whether the asymptotic state is reached in a finite time unless one knows the connectivity properties of the phase space, which in our case corresponds to know $D(\rho)$.

IV. EDWARDS' ASSUMPTION

Before considering the finite-dimensional models let briefly discuss more deeply the meaning of Edwards' assumption. One possibility of making an assumption à la Edwards would be to consider a fast quench, and then propose that the configuration reached has the macroscopic properties of the typical blocked configurations. This would imply that the system stops at a density for which the number of blocked configurations is maximal. We do not follow this path, as we will give sufficient evidence that generically the vast majority of the blocked configurations are much less compact than the one reached dynamically, even after abrupt quenches.

Our strategy here is instead to quench the system to a situation of very weak but non-zero tapping, shearing or thermal agitation. In this way, the system keeps compactifying, albeit at a very slow rate. In this context, we consider a flat measure over blocked configurations *conditioned to having the energy and/or density of the dynamical situation we wish to reproduce.* We do not follow this path, as we will give sufficient evidence that generically the vast majority of the blocked configurations are much less compact than the one reached dynamically, even after abrupt quenches.

Our strategy here is instead to quench the system to a situation of very weak but non-zero tapping, shearing or thermal agitation. In this way, the system keeps compactifying, albeit at a very slow rate. In this context, we consider a flat measure over blocked configurations *conditioned to having the energy and/or density of the dynamical situation we wish to reproduce.* This means that we have given up trying to predict the dynamical energy or density by methods other than the dynamics itself.

That configurations with low mobility should be relevant in a jammed situation is rather evident, the strong hypothesis here is that the configurations reached dynamically are *the typical ones* of given energy and density. Had we restricted averages to blocked configurations having *all* macroscopic observables coinciding with the dynamical ones, the construction would exactly, and trivially, reproduce the dynamic results. The fact that conditioning averages to the observed energy and density suffices to give, at least as an approximation, other dynamical observables is highly non-trivial. A natural a puzzling question arises. Is it reasonable to use blocked configurations as a distribution for the dynamic situation? This seems odd, since we know that neither a relaxing nor a gently driven system will stay in one of those configurations! Here the example of the stationary measure in dynamic systems is instructive: we know that such a measure can be constructed by considering only the periodic trajectories, although the probability that the system is *in* a periodic trajectory is strictly zero. Somehow, these trajectories form a 'skeleton' of the true distribution — and such would also be the role of the blocked configurations in Edwards' measure. W have anyway checked that configurations with a small, though non-zero fraction of mobile particles yield the same statistics.

V. KA MODEL

The first model we consider is the so-called Kob-Andersen (KA) model [18] that was first studied in the context of Mode-Coupling theories [38] as a finite dimensional model exhibiting a divergence of the relaxation time at a finite value of the control parameter (here the density); this divergence is due to the presence in this model of the formation of "cages" around particles at high density (the model was indeed devised to reproduce the cage effect existing in super-cooled liquids).

Though very schematic, it has then been shown to reproduce rather well several aspects of glasses [39], like the aging behaviour with violation of FDT [40], and of granular compaction [41].

The simplicity of its definition and the fact that it is non mean-field makes it a very good candidate to test Edwards' ideas: in fact, the triviality of its Gibbs measure will allow us to compare the numerical data obtained for the dynamics and for Edwards' measure with the analytic results for equilibrium.

A. Definition

The model is defined as a lattice gas on a three dimensional lattice, with at most one particle per site. The dynamical rule is as follows: a particle can move to a neighboring empty site, only if it has strictly less than m neighbors in the initial and in the final position. Following [18], we take $m = 4$: this ensures that the system is still ergodic at low densities, while displaying a sharp increase in relaxation times at a density well below 1. The dynamic rule guarantees that the equilibrium distribution is trivially simple since all the configurations of a given density are equally probable: the Hamiltonian is just 0 since no static interaction exists.

In order to mimic a compaction (or aging) process without gravity, we simulate a 'piston' by creating and destroying particles only on the topmost layer (of a cubic lattice of linear size L) with a chemical potential μ [39]. More precisely, each Monte-Carlo sweep is divided in the following steps: (i) for each of the site of the topmost layer, add a particle if the site is empty, and, if it is occupied, withdraw the particle with probability $\exp(-\beta\mu)$. (ii) try to move each particle, in random order, according to the dynamical rule.

B. Gibbs measure

Since the Hamiltonian is 0, the equilibrium (or Gibbs) measure corresponds simply to a flat measure over all configurations, without taking into account the dynamical constraint. Therefore, the relation between density and chemical potential is

$$\rho = \frac{1}{1+\exp(-\beta\mu)} \ , \tag{23}$$

and the exact equilibrium entropy density reads

$$s_{equil}(\rho) = -\rho\ln\rho - (1-\rho)\ln(1-\rho) \, . \tag{24}$$

with in particular

$$\frac{ds_{equil}}{d\rho} = -\beta\mu \, . \tag{25}$$

In this model, the temperature $1/\beta$ is irrelevant since it appears only as a factor of the chemical potential and we can set it to one throughout.

Besides, the equilibrium structure factor defined as the probability that two sites at distance r are both occupied is easily seen to be a constant

$$g_{equil}(r) = \rho^2 \quad ; \quad r > 0 \tag{26}$$

No correlations appear since the configurations are generated by putting particles at random on the lattice. It will therefore be easy, as already mentioned, to compare small deviations from $g_{equil}(r)$, a notoriously difficult task to do in glassy systems. Note that it is also easy to numerically sample Gibbs' measure at any given density, by simply generating at random configurations with fixed number of particles.

C. Non-equilibrium dynamics

The previously described Monte-Carlo procedure allows to produce equilibrium configurations, even if the dynamical constraint is enforced, as long as μ is low enough. However, at densities close to ρ_g ($\simeq 0.88$), the particle diffusion becomes extremely slow due to the kinetic constraints. In fact, the diffusion coefficient is well approximated by

$$D(\rho) \sim (\rho_g - \rho)^{\phi}\,, \tag{27}$$

with $\phi \simeq 3.1$ [18]. The equilibrium with $\rho > \rho_g$ is not reached by compaction after extremely long times: if a chemical potential μ such that $\rho(\mu) > \rho_g$ is applied, the system falls out of equilibrium. Moreover, the density obtained at long times depends on the history: the slower the chemical potential is raised, the denser the system becomes [39].

We are here interested in this out of equilibrium dynamics: we therefore perform a compression, starting from low density, by raising the chemical potential up to a high value $\mu = 3$. Since the equilibrium density at $\mu = 3$ is much larger than the jamming density ρ_g, aging and very slow compaction ensue. We record the density $\rho(t)$, the density of mobile particles $\rho_m(t)$, and the spatial structure function $g_{dyn}(r,t)$ defined as the probability that two sites at distance r are occupied. Since we work at finite sizes, and since particles are always added at the same layer, density heterogeneities do appear between the topmost layer and the rest of the box if the compression is too fast. To avoid any systematic error, we use a slow compression ($\Delta t = 10^4$ MC sweeps for each increase of $\Delta\mu = 0.01$), and we measure the various quantities in the center of the box only, where we checked that the system is indeed homogeneous.

We show in Fig. 2 the parametric plot $\rho_m(t)$ versus $\rho(t)$; at short times and low density, it follows the equilibrium curve (obtained by generating at random configurations of density ρ and thus measuring the mean density of mobile particles for the Gibbs measure); at low μ indeed, the relaxation time of the system is smaller than the rate of increase of μ, so the system has time to equilibrate. As the density approaches ρ_g however, compaction slows down and $\rho_m(t)$ gets smaller. At large times the system is approaching ($\rho \sim \rho_g, \rho_m \sim 0$).

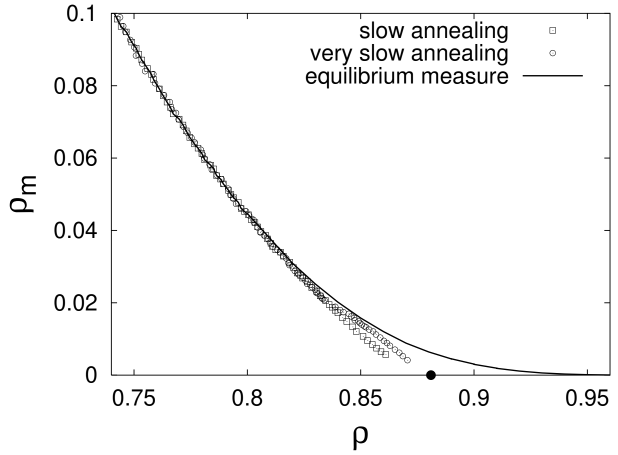

FIG. 2. Parametric plot of the density of mobile particles versus the density, for the equilibrium measure (data obtained by generating at random configurations of a given density and measuring the number of mobile particles), and during two compaction procedures (with $\Delta\mu/\Delta t = 10^{-5}$ and 10^{-6}).

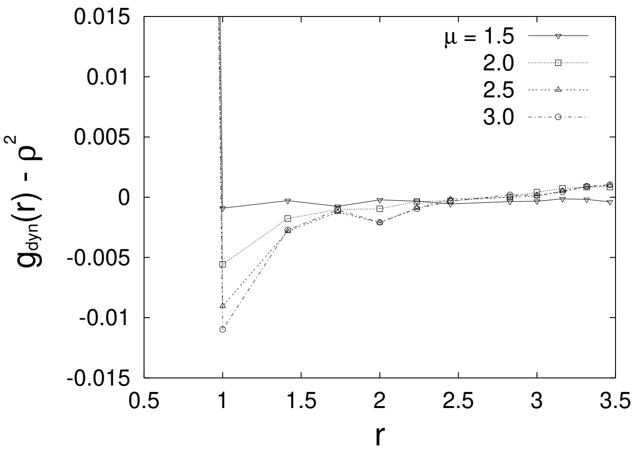

FIG. 3. Dynamic structure function obtained in a very slow compression, at different times, i.e. different values of μ; at $\mu = 1.5$ the system is still at equilibrium and the correlation function is therefore equal to g_{equil}, but stronger and stronger deviations are observed as μ is raised.

We have also measured the dynamical structure function $g_{dyn}(r,t)$, displayed in Fig. 3; induced and spontaneous displacements were measured and compared in [40], and these data will be displayed and used in section III-F.

D. The auxiliary model

We introduce an 'auxiliary model' which will allow us to define the Edwards measure for the KA model. In this model particles have energy equal to one if the dynamic rule of the KA model allows them to move, and to zero otherwise. The Hamiltonian is therefore highly complicated, involving next-nearest neighbor interactions. We can however introduce an auxiliary temperature $1/\beta_{aux}$ associated to the auxiliary energy E_{aux} (equal to the number of particles that are able to move) and perform a simulated annealing, at fixed number of particles: at low β_{aux} all configurations are sampled uniformly, while, as β_{aux} grows, the sampling is restricted to configurations with vanishing fraction of moving particles. The Monte Carlo procedure uses non-local moves (accepted with a standard Metropolis probability $\min\{1, \exp(-\beta_{aux}\Delta E_{aux})\}$) which allow for an efficient sampling: these non-local moves have nothing to do with the true dynamics of the original model, and therefore the auxiliary model is not glassy..

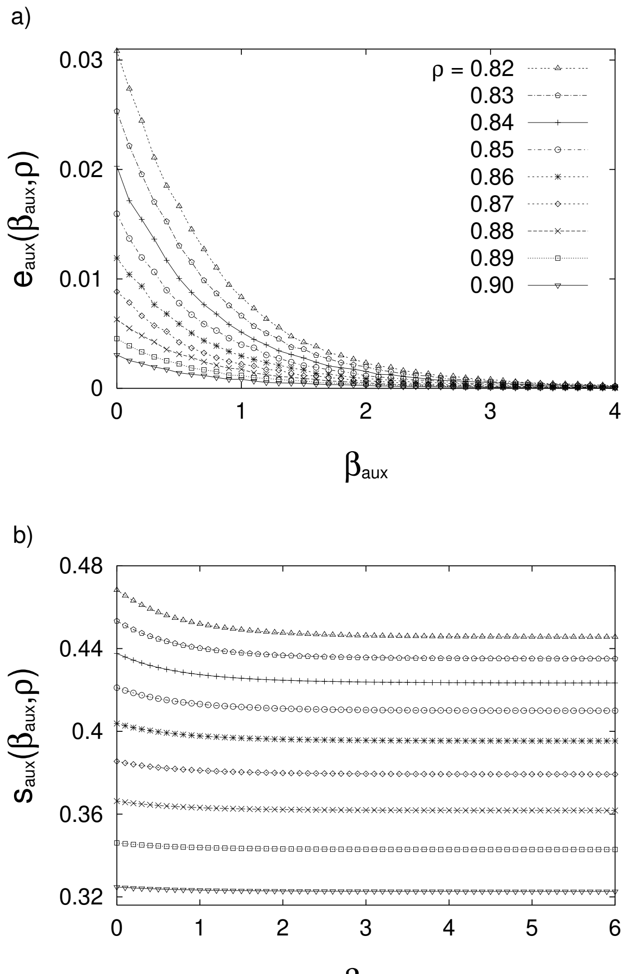

FIG. 4. Thermodynamical properties of the auxiliary model. a) Energy density e_{aux} vs. inverse temperature β_{aux} at different particle density ρ. b) Entropy density s_{aux} as obtained from thermodynamic integration of the energy data.

In this way, we obtain the equilibrium energy density of the auxiliary model, $e_{aux}(\beta_{aux}, \rho)$ and its entropy density $s_{aux}(\beta_{aux}, \rho)$ by thermodynamic integration:

$$s_{aux}(\beta_{aux}, \rho) = s_{equil}(\rho) + \beta_{aux}\, e_{aux}(\beta_{aux}, \rho)$$

$$- \int_0^{\beta_{aux}} e_{aux}(\beta'_{aux}, \rho)\, d\beta'_{aux}\,. \qquad (28)$$

where we set

$$s_{aux}(0, \rho) = s_{equil}(\rho) \qquad (29)$$

since the limit $\beta_{aux} \to 0$ corresponds to the equilibrium measure. In fig. 4 we show a subset of data concerning the energy and entropy densities of the auxiliary model. (The energy has been computed in the range $\rho \in [0.65, 0.95]$ with a step in density $\Delta\rho = 0.005$ and for $\beta_{aux} \in [0, 20]$ with step $\Delta\beta_{aux} = 0.1$).

We also evaluate the structure function of the auxiliary model $g_{aux}(r, \beta_{aux})$ which is shown in fig. 5 for a density $\rho = 0.87$. It is clear here as well as in fig. 4 that the limit $\beta_{aux} \to \infty$ considered in the next subsection is already approached for $\beta_{aux} \simeq 5$.

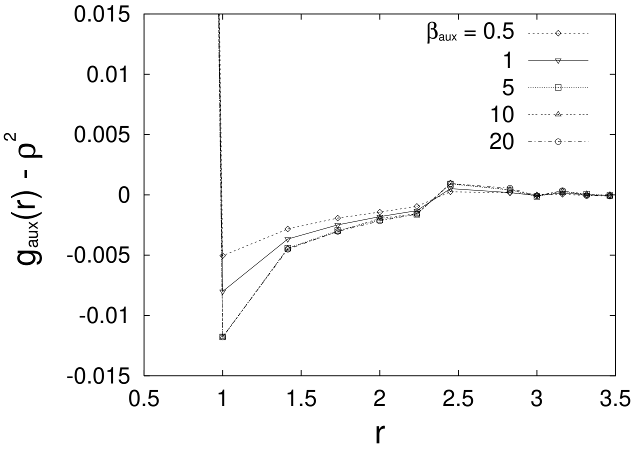

FIG. 5. Structure function obtained in the auxiliary model at different values of the temperature β_{aux} and for a density $\rho = 0.87$. The data for $\beta_{aux} = 5$, 10 and 20 are indistinguishable.

E. Edwards measure

To evaluate the observables with Edwards' measure, i.e. the set of configurations where all particles are unable to move, we consider now the limit $\beta_{aux} \to \infty$ of the observables computed in the auxiliary model. For example, the Edwards entropy is then obtained as

$$s_{Edw}(\rho) \equiv \lim_{\beta_{aux}\to\infty} s(\beta_{aux}, \rho)$$

$$= s_{equil}(\rho) - \int_0^{\infty} e_{aux}(\beta'_{aux}, \rho)\, d\beta'_{aux}\,, \qquad (30)$$

since

$$\lim_{\beta_{aux}\to\infty} \beta_{aux}\, e_{aux}(\beta_{aux}, \rho) = 0\,. \qquad (31)$$

In fig. 6 we plot the Edwards and the equilibrium entropy as a function of the particle density.

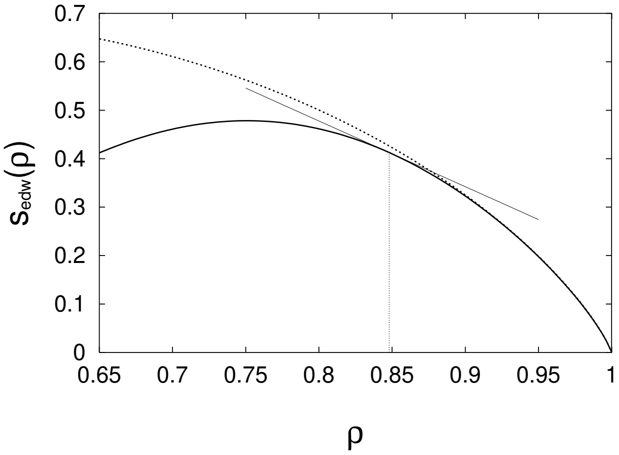

FIG. 6. Edwards entropy density of the Kob-Andersen model vs. density (full curve). For comparison we also show the equilibrium entropy (dashed curve). At high enough density the curves are indistinguishable, and join exactly only at $\rho = 1$. The slope of the tangent to $s_{Edw}(\rho)$ for a generic ρ allows to extract $T_{Edw}(\rho)$ from the relation $T_{Edw}(\rho)\frac{ds_{Edw}}{d\rho} = \frac{ds_{equil}}{d\rho}$.

Comparison of Fig. 6 with Fig. 2 shows that the most typical blocked configurations ($\rho \sim 0.75$) are irrelevant as far as the compaction dynamics is concerned.

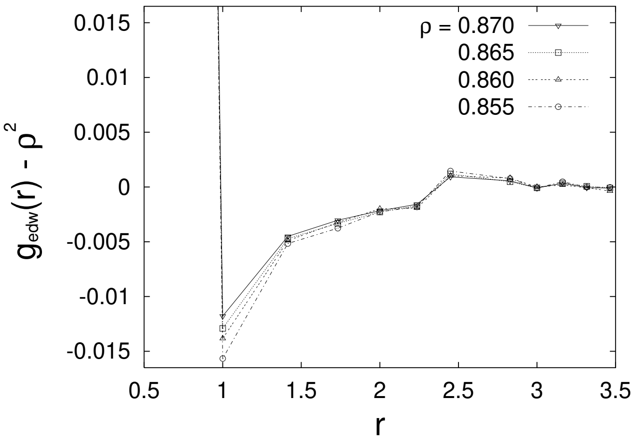

FIG. 7. Edwards structure function $g_{Edw}(r)$ obtained as limit of the $g_{aux}(r, \beta_{aux})$ for $\beta_{aux} \to \infty$. As the density increases the deviation from g_{equil} gets less pronounced.

Since the relation between chemical potential, temperature and entropy density at equilibrium is given by (25), the natural definition for Edwards' temperature is

$$T_{Edw}^{-1} = -\frac{1}{\mu}\frac{ds_{Edw}(\rho)}{d\rho}\,. \tag{32}$$

However we work here at fixed density for Edwards' measure, and we therefore compute:

$$T_{Edw} = \frac{\frac{ds_{equil}(\rho)}{d\rho}}{\frac{ds_{Edw}(\rho)}{d\rho}} \tag{33}$$

Similarly, the Edwards measure structure function, $g_{Edw}(r)$, is obtained as

$$g_{Edw}(r) = \lim_{\beta_{aux}\to\infty} g_{aux}(r, \beta_{aux})\,. \tag{34}$$

and displayed in fig.7 for various densities.

Two remarks are in order

- as the density approaches 1, almost all particles become blocked even for Gibbs' measure; more precisely, $\lim_{\rho\to 1} \rho_m^{Gibbs} = 0$; thus, Edwards' and Gibbs' measures get closer, which is seen in fig. 6 by the fact that the curves for s_{equil} and s_{Edw} get very close, and $\lim_{\rho\to 1} T_{Edw} = T_{Gibbs} = 1$. Similarly, $g_{Edw}(r)$ deviates less from g_{equil} as ρ increases, as is shown in Fig. 7.
- Edwards' measure is precisely defined as a sampling over configurations with vanishing fraction of mobile particles. We mention here for completeness the straightforward generalization of Edwards' measures as the set of configurations with fraction of mobile particles *smaller than* ϵ (cfr. the quasi-states of [27]); we then can use the knowledge of $e_{aux}(\beta_{aux}, \rho)$ to define β^ϵ as the value of the auxiliary temperature such that $e_{aux}(\beta^\epsilon, \rho) = \epsilon$, and thus define

$$\begin{aligned} s_{Edw}^{\epsilon}(\rho) &\equiv s(\beta_{aux} = \beta^\epsilon, \rho) \\ &= s_{equil}(\rho) + \epsilon\,\beta^\epsilon \\ &\quad - \int_0^{\beta^\epsilon} e_{aux}(\beta_{aux}, \rho)\, d\beta_{aux}\,. \end{aligned} \tag{35}$$

It is clear that $s_{Edw}^1 = s_{equil}$, while $s_{Edw}^0 = s_{Edw}$. We can also measure the structure factors $g^\epsilon(r) \equiv g(r, \beta^\epsilon)$.

F. Comparing the measures

We are now in a position to compare the long-time results of the out of equilibrium dynamics with those obtained with the different measures. Section II-C has already made clear that the equilibrium measure is not able to describe these results. Fig. 8 shows a plot of the mobility

$$\chi(t, t_w) = \frac{1}{3N}\sum_{a=1}^{3}\sum_{k=1}^{N}\frac{\delta\left\langle (r_k^a(t) - r_k^a(t_w))\right\rangle}{\delta f}\,, \tag{36}$$

obtained by the application of random forces to the particles (see [40] for details), *vs.* the mean square displacement

$$B(t, t_w) = \frac{1}{3N}\sum_{a=1}^{3}\sum_{k=1}^{N}\left\langle (r_k^a(t) - r_k^a(t_w))^2\right\rangle, \tag{37}$$

testing in the compaction data the existence of a dynamical temperature T_{dyn} [40]. (N is the number of particles and a runs over the spatial dimensions) One first remarks the existence of a dynamical temperature T_{dyn}. Furthermore the agreement between T_{dyn} and T_{Edw}, obtained from the blocked configurations as in Fig. 6, for the density at which the dynamical measurement were made, is clearly excellent.

In Fig. 9 we plot the long-time dynamical $g_{dyn}(r,t)$, the equilibrium $g_{equil}(r) = \rho^2$, and the Edwards' $g_{Edw}(r)$ structure factors, for the same density $\rho \sim 0.87$. While $g_{equil}(r)$ is flat, the system has developed during its dynamical evolution some structures, which seem to be reproduced rather well by $g_{Edw}(r)$. Note that using the generalized Edwards' measures does not improve the agreement in a clear-cut way because of the rather large error-bars on the dynamical data.

To summarize, during the compaction, the system falls out of equilibrium at high density, and is therefore no more described by the equilibrium measure. It turns out that Edwards' measure, constructed by a flat sampling of the blocked configurations at the dynamically reached density, reproduces the physical quantities measured at large times, and in particular predicts the correct value for the dynamical temperature.

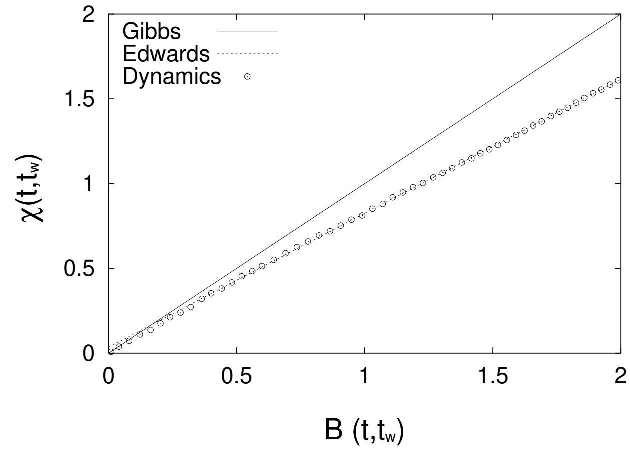

FIG. 8. Einstein relation in the Kob-Andersen model: plot of the mobility $\chi(t,t_w)$ vs. the mean-square displacement $B(t,t_w)$ (data shown as circles). The slope of the full straight line corresponds to the equilibrium temperature ($T=1$), and the slope of the dashed one to Edwards' prescription obtained from figure 6 at $\rho(t_w) = 0.848$.

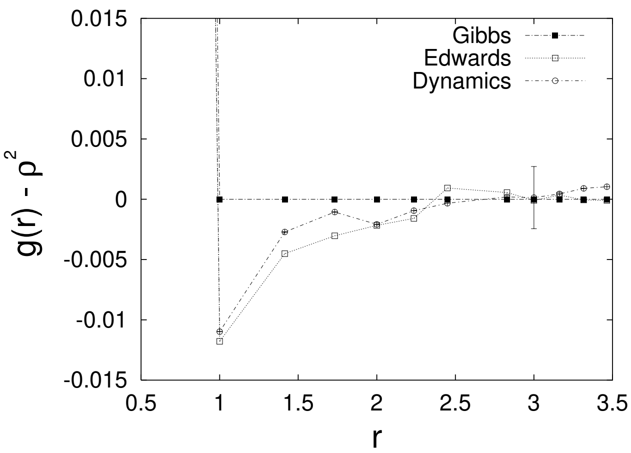

FIG. 9. Structure functions $g(r) - \rho^2$ at density $\rho \simeq 0.87$ computed with the equilibrium, Edwards' and dynamical measure of the Kob-Andersen model. The three sets of data come from independent Monte-Carlo simulations. The dynamic structure function (circles) is obtained after a very slow compression by raising the chemical potential from $\mu = 1$ to $\mu = 3$ with an annealing rate of 10^{-6} Monte Carlo sweeps. The Edwards' structure function (open squares) is obtained from the auxiliary model. Although the equilibrium value of $g(r) - \rho^2$ is exactly 0, we also obtain it by a Monte-Carlo simulation (full squares) in order to show that the difference in the short distance behaviour is not an artifact of the numerical simulation). The size of the typical error bar on dynamical data is shown at $r = 3$.

VI. TETRIS MODEL

In this section we extend the results obtained for the KA model to another class of models, the so-called Tetris Model (TM) [19]. We proceed as before by constructing explicitly Edwards' and Gibbs' measures, together with the corresponding entropy and expectation values of some observables, and comparing both sets of data with those obtained with an irreversible compaction dynamics. Notice that in this case the equilibrium measure is by no means trivial and it has to be computed numerically, using an auxiliary model as for the construction of Edwards' measure.

A. Model Definition

The essential ingredient of the TM [19] is the geometrical frustration that for instance in granular packings is due to excluded volume effects arising from different shapes of the particles. This geometrical feature is captured in this class of lattice models where all the basic properties are brought by the particles and no assumptions are made on the environment (lattice). The interactions are not spatially quenched but are determined in a self-consistent way by the local arrangements of the particles. It is worth to notice how in this class of models the origins of the randomness and of the frustration coincide because both are given in terms of the particle properties.

Despite the simplicity of their definition, these systems are able to reproduce many general features of granular media: the very slow density compaction [19], segregation phenomena [37], dilatancy properties [42] as well as memory [9] and aging [6,7].

Let us recall briefly the definition of the model, which includes, like in the real computer game *Tetris*, a rich variety of shapes and sizes. On a lattice each particle can be schematized in general as a cross with 4 arms (in general the number of arms is equals to the coordination number of the lattice) of different lengths, chosen in a random way. An example of particle configuration on a square lattice is shown in Fig. 10.

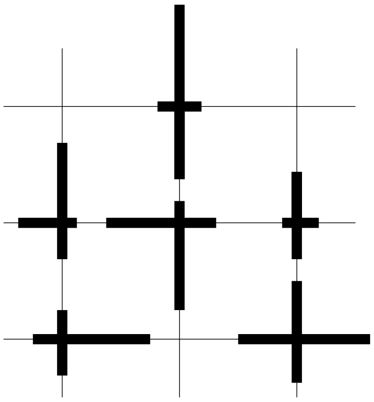

FIG. 10. Sketch of a local arrangement of particles in the Tetris Model: each particle can be schematized in general as a cross with 4 arms of different lengths, chosen in a random way.

The interactions among the particles obey the general rule that one cannot have superpositions. For instance one has to check that for two nearest-neighbor particles the sum of the arms oriented along the bond connecting the two particles is smaller than the bond length. It turns out that in this way the interactions between the particles are not fixed once for all but they depend on the complexity of the spatial configuration.

The extreme generality of the model definition allows a large variety of choices for the particles. While the original model deals with simple rods, the fact that these rods can arrange in an antiferromagnetic-like configuration of density 1 has motivated the use of random shapes to avoid this pathology. In this study, on the other side, we will use the so-called "T"-shaped particles defined in such a way that three arms have length equal to $\frac{3}{4}d$ and the fourth one zero length. d sets the bond size on the square lattice. With this definition one has four types of particles corresponding to the four possible orientation of the "T"s on a square lattice. Our choice has the following advantages: on the one hand, no averaging over the disorder is needed; on the other hand, the process of applying a chemical potential together for particles of various sizes could produce a 'filtering' effect that would dynamically lead to an artificially dense system with only small particles. With the above given rules one can define the allowed configurations. One can easily realize how the maximal allowed density is equal to $\rho_{max} = \frac{2}{3}$ which corresponds to a number of possible configurations proportional to the linear size of the lattice, L (due to the possible translations and symmetries). Fig. 11 shows two possible configurations with $\rho = \rho_{max}$.

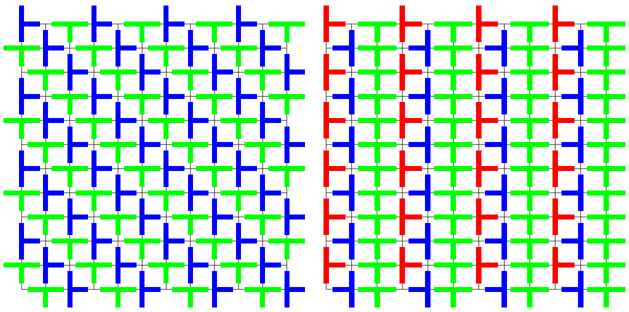

FIG. 11. Two possible configurations of the Tetris model considered with the maximal density $\rho = \rho_{max} = 2/3$.

B. Equilibrium measure

The equilibrium measure is obtained with an annealing procedure. We can introduce a temperature $T = 1/\beta$ associated with an energy E defined as the total particle overlaps existing in a certain configuration. For each value of T one allows the configurations with a probability given by $e^{-\beta E}$. Starting with a large temperature T (a very small β) one samples the allowed configurations by progressively decreasing T (increasing β). As T is reduced E decreases and only at $T = 0$ (no violation of constraints allowed) the energy is precisely zero. The exploration of the configuration space can be performed in two ways:

1) working at constant density by interchanging the positions of couples of particles. This procedure is used to compute $E(\beta, \rho)$ and $e(\beta, \rho)$ (energy density), from which one can compute the equilibrium entropy density by the expression:

$$s_{equil}(\rho) \equiv s_{equil}(\beta = \infty, \rho) = \\ = s_{equil}(\beta = 0, \rho) - \int_0^\infty e(\beta, \rho) d\beta \quad (38)$$

For the choice made for the particles one has

$$s_{equil}(\beta = 0, \rho) = -\rho \ln \rho - (1 - \rho) \ln(1 - \rho) \\ +\rho \ln 4, \quad (39)$$

which is easily obtained by counting the number of ways in which one can arrange ρL^2 particles of four different types on $N = L^2$ sites;

2) working at constant chemical potential μ by adding and removing particles. In this case the density fluctuates and one measures $E(\beta, \mu)$.

In both cases one can measure the particle-particle correlation function (equivalent to the void-void correlation function) $g_{equil}(r)$. Since, working at constant μ the density fluctuates, we have always measured directly the ensemble average $< (g_{equil}(r) - \rho^2) >$ in order to make the data obtained with the two different methods comparable. One can then compare the correlation function obtained at constant μ (which corresponds to a certain average density) with the correlation function obtained working at constant density. The results of both methods are equivalent.

Fig.s (12) and (13) report the results for $e(\beta, \rho)$ and $s_{equil}(\rho)$ as obtained from (38).

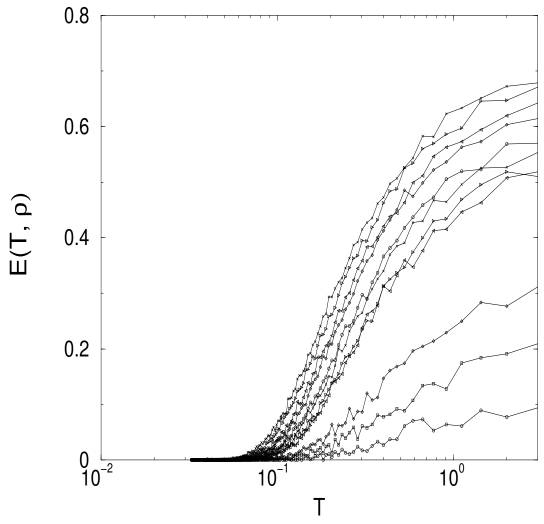

FIG. 12. $e(\beta = 1/T, \rho)$ for various values of ρ. From top to bottom the density decreases monotonically from $\rho = 0.6$ to $\rho = 0.1$

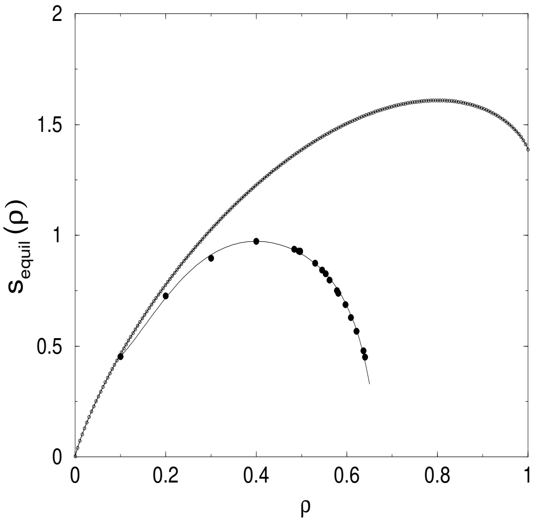

FIG. 13. Entropy density in equilibrium $s_{equil}(\rho)$ and, for reference, entropy density at $T_{aux} = \infty$. $s_{equil}(\rho)$ goes to zero at $\rho = \frac{2}{3}$.

Fig. 14 reports the results for $< (g_{equil}(r) - \rho^2) >$ for different values of ρ. The correlation functions g (g_{equil} or g_{Edw} or g_{dyn}) actually display oscillations around ρ^2, whose origin can be easily understood: if a particle occupies a site, the exclusion rules decreases the probability that a neighboring site will be occupied. We therefore plot in the figures $< (g(r) - \rho^2) >^2$ in order to show the exponential decay of the correlations.

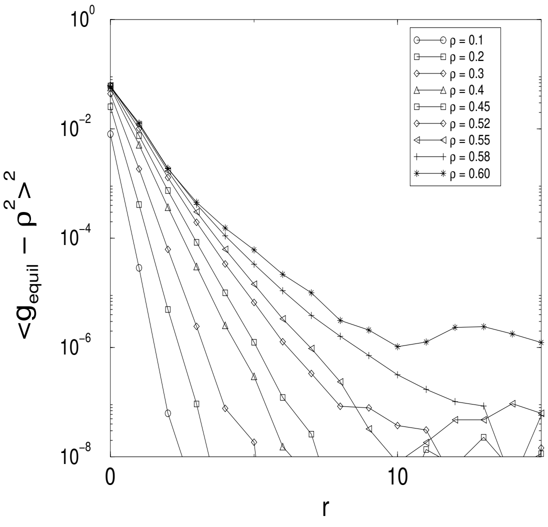

FIG. 14. $< (g_{equil}(r) - \rho^2) >^2$ for various values of ρ. From top to bottom the density decreases monotonically from $\rho = 0.64$ to $\rho = 0.1$.

C. Edwards' measure

Edwards' measure is obtained with an annealing procedure at fixed density. This means that one samples the configurational space by interchanging the positions of couples of particles without violations of constraints. In this way one is sampling the configurational space corresponding already to $T = 0$. In order to select only the subset of configurations contributing to the Edwards' measure we introduce an auxiliary temperature T_{aux} (and the corresponding $\beta_{aux} = 1/T_{aux}$) and, associated to it, an auxiliary energy E_{aux} which, for each configuration, is equal to the number of mobile particles, in the same way as for the KA model. A particle is defined as mobile if it can be moved according to the dynamic rules of the original model.

Let us describe in detail how the measurements are performed. Since for each given density one is interested in the subset of the equilibrium configurations with a reduced particle mobility, we start with an annealing procedure precisely identical to the one used for the equilibrium measure. This procedure allows us to reach a starting configuration with a given density and no constraints violated. At this stage we perform a Monte Carlo procedure which exchanges the positions of couples of particles without violation of constraints: this procedure accepts the non-local moves with a standard Metropolis probability $\min(1, \exp(-\beta_{aux}\Delta E_{aux}))$ which allow for an efficient sampling. These non-local moves define an auxiliary dynamics which has nothing to do with the true dynamics of the original model, and therefore the auxiliary model is not glassy.

As for the equilibrium we have performed a certain set of measures.

In particular we have measured $E_{aux}(\beta_{aux}, \rho)$, i.e. the decrease of the auxiliary energy at fixed density. In order to do this one performs an annealing procedure increasing progressively β_{aux} and monitoring for each β_{aux} the corresponding configurational energy $E_{aux}(\beta_{aux}, \rho)$. From this measure one can compute the Edwards' entropy density defined by:

$$\begin{aligned} s_{Edw}(\rho) &\equiv s_{aux}(\beta_{aux} = \infty, \rho) = \\ &= s_{equil}(\rho) - \int_0^{\infty} e_{aux}(\beta_{aux}, \rho) d\beta_{aux} \end{aligned} \qquad (40)$$

where $e_{aux}(\beta_{aux}, \rho)$ is the auxiliary Edwards' energy density and we put $s_{equil}(\rho) = s_{aux}(\beta_{aux} = 0, \rho)$.

Fig. 15 reports the results for $s_{Edw}(\rho)$ as obtained from (40) compared with $s_{equil}(\rho)$.

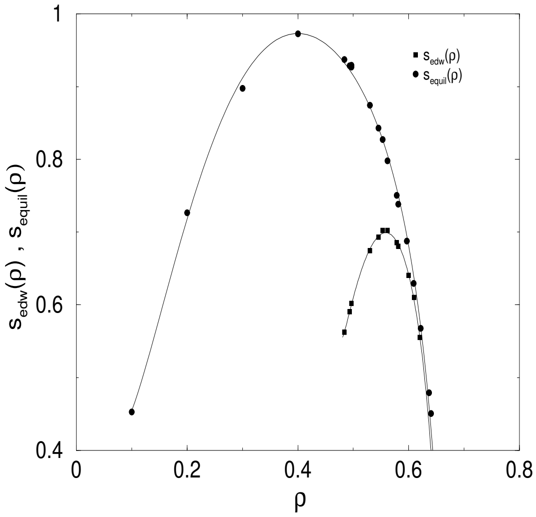

FIG. 15. Edwards' entropy density, $s_{Edw}(\rho)$ and equilibrium entropy density, $s_{equil}(\rho)$. Both go to zero at $\rho = \frac{2}{3}$.

For the computation of the particle-particle correlation function we have to use a different strategy. Always starting from a configuration with a given density and no constraints violated one performs a Monte Carlo procedure, at β_{aux} fixed, which exchanges the positions of pairs of particles without violation of constraints. Each single simulation uses ρ and β_{aux} as input parameters. In practice one is trying to sample all the configuration of density ρ and with a particle mobility defined by β_{aux}. In this context the Edwards' prescription should correspond to the limit $\beta_{aux} \to \infty$. In this way we have computed $< (g_{Edw}(r) - \rho^2) >$ for several values of β_{aux} and we report the results in Fig. 16. As one can see the limit $\beta_{aux} \to \infty$ is attained already for β_{aux} of the order of 6.

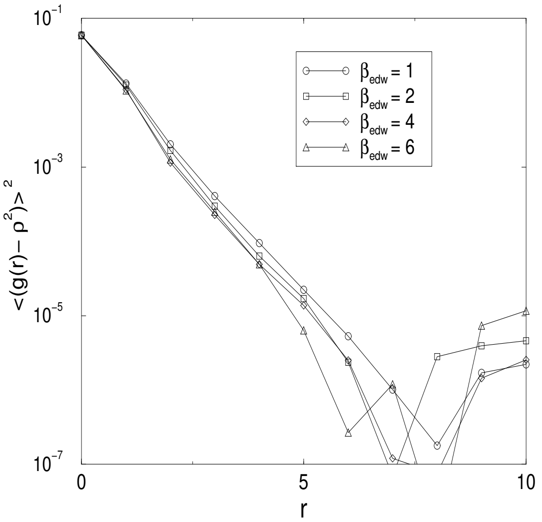

FIG. 16. $< (g_{Edw}(r) - \rho^2) >^2$ for $\rho = 0.58$; $\beta_{aux} = 1, 2, 4, 6$. The behaviour seems to saturate to a limit that should correspond to $\beta_{aux} \to \infty$ already for β_{aux} of the order of 6.

D. Irreversible Compaction Dynamics

We now turn to the out of equilibrium dynamics of compaction, simulated by starting from an empty lattice and performing N steps of attempted particle additions followed by M steps of attempted particle diffusions. Fig. 17 reports the results for the density increase and for the fraction of mobiles particles as a function of the density for $N = 1, M = 1$ and $N = 10, M = 1$. While the limit $N =$ fixed $M- > \infty$ should coincide with the equilibrium, it is clear that the system, at finite M, is not able to approach its maximum density and falls out of equilibrium. Here again the density at which the number of blocked configurations is maximal is smaller than the one achieved by compaction.

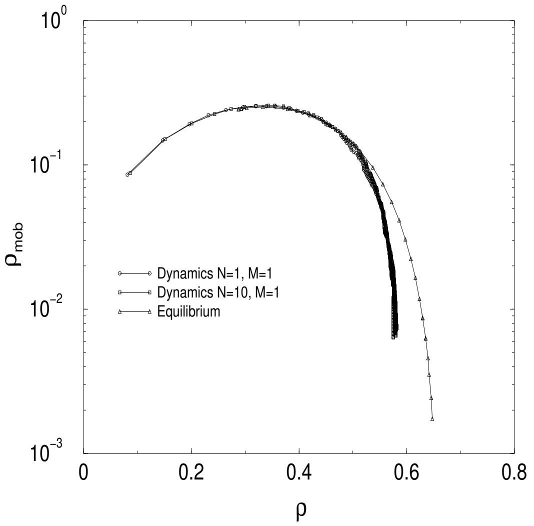

FIG. 17. ρ_{mob} vs. ρ for two irreversible dynamics with $N = 1, M = 1$ and $N = 10, M = 1$. For reference is plotted the equilibrium curve.

It is particularly interesting to notice that in the out-of-equilibrium configurations visited during the irreversible dynamics the fraction of mobile particles ρ_{mob} at fixed density is systematically smaller than the corresponding value in equilibrium. This suggests the possibility of distinguishing between equilibrium and out-of-equilibrium configurations by looking at the spatial organization of the particles in both cases. We have then measured, during the compaction dynamics, the particle-particle correlation function at fixed density. In the next section we shall compare these results with those obtained on the basis of the equilibrium and Edwards' measures.

E. Comparing different measures

We are now able, as for the KA model, to compare Gibbs' and Edwards' measures with the results of the out-of–equilibrium dynamics at large times.

In Fig. 18 we plot the deviations of the particle-particle correlation functions from the uncorrelated value ρ^2. In particular we compare $< (g_{dyn}(r) - \rho^2) >^2$ obtained during the irreversible compaction ($N = 1, M = 1$) with the corresponding functions obtained with the equilibrium and Edwards' measures. It is evident that the correlation function, as measured during the irreversible compaction dynamics, is significantly different from the one obtained with the equilibrium measure. On the other hand the correlation functions obtained with Edwards' measure are able to better describe what happens during the irreversible dynamics. In particular what is observed is that the correlation length seems to be smaller for configurations explored by the irreversible dynamics than in the equilibrium configurations. This aspect is captured by Edwards' measure which selects, the better the larger β_{aux}, configurations with a reduced particle mobility. In practice one can summarize the problem as follows: given a certain density, one can arrange the particles in different ways. The different configurations obtained in this way differ in the particle mobility and this feature is reflected by the change in the particle-particle correlation properties.

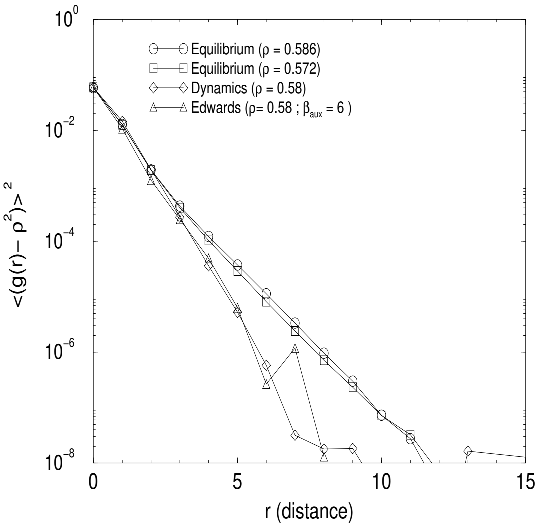

FIG. 18. Comparison between the correlation functions obtained with the equilibrium measure, the Edwards measure ($\beta_{aux} = 6$) and the irreversible dynamics ($N = 1, M = 1$). In all cases the system is considered at a density of $\rho \simeq 0.58$.

Also in this case, as in the KA example, it turns out that Edwards' measure, constructed by a flat sampling of the blocked configurations, is able to reproduce the physical quantities measured at large times. Preliminary results confirms that also in the Tetris model the temperature predicted with the Edwards' approach coincide with the dynamical temperature T_{dyn} as defined for the KA model [43].

VII. CONCLUSIONS

A few remarks are in order.

The connection of Edwards' ensemble with the dynamical FDT temperature immediately suggests experiments to check the validity of these ideas, for example by studying diffusion and mobility of different tracer particles within driven granular media.

At present, the correspondence between Edwards' distribution and the long-time dynamics is at best checked but does not follow from any known principle. Now that several concrete examples have lent credibility to Edwards' construction, an effort to understand why it does in some cases work and what is its range of validity has become worthwhile.

Finally it is important to warn the reader about a misconception about Edwards's hypothesis. It goes like this: *The system has at every energy and density many blocked configurations. Now, we know that in systems with many minima (for example from mean-field glasses) all the minima of given energy tend to have the same values for macroscopic observables. Hence, it is natural to assume that their basins of attraction are themselves also the same, and hence Edwards' 'flat average' assumption is justified.*

To see the danger of such a reasoning, let us paraphrase it in another context, in which it is clear that the conclusion is generically erroneous: consider a *driven, macroscopic system* [44] (e.g. fully developed turbulence) thermostated at energy E. By the same token, we would say: *The system is restricted to move in the energy $= E$ shell. Now, we know that almost all points in an energy shell of a macroscopic system have in the thermodynamic limit the same values of macroscopic observables (we disregard symmetry breaking cases). Hence, it is natural to suppose that the dynamic stationary measure is also the same in all points: therefore the stationary distribution is flat, i.e. microcanonical.*

This is of course wrong: we know that generically the stationary measure of a driven, thermostated system is dominated by an ensemble of zero volume within the energy shell. Almost all points in the energy shell do have the same weight, *but this weight is zero.* In order that the stationary measure coincides with the microcanonical measure we need some strongly specific properties for the dynamics: such is the case of chaotic *Hamiltonian* dynamics. The same can be said about Edwards' measure: that all blocked configurations of a given energy have the same basin of attraction may be quite generally true, but in order for Edwards' measure to be relevant the combined basin of attraction of the typical configurations should not vanish!

Starting from a random configuration the probability of falling into a basin is proportional to its volume, so with a quench we are not sampling a typical basin: rare basins (exponentially smaller in quantity) of large (exponential) volume may dominate — and this is generally true for a quench from equilibrium at any temperature. Using Edwards' measure is justified when for some reason one can consider that typical basins of a given level are also typically accessed: a very strong assumption that is generally not valid. The reason this hypothesis (if true) is useful is that one can construct averages over configurations defined by a local property (being blocked) without having to know the basin of attraction, which involves solving the dynamics.

This work has also been partially supported from the European Network-Fractals under contract No. FM-RXCT980183.

[1] E. Caglioti and V. Loreto, *Phys. Rev. Lett.* **83**, 4333 (1999).
[2] A. Barrat, J. Kurchan, V. Loreto and M. Sellitto, *Phys. Rev. Lett.* **85** 5034 (2000).
[3] A. Barrat, J. Kurchan, V. Loreto and M. Sellitto, *Phys. Rev. E* **63**, 051301-1 (2001).
[4] H.M. Jaeger, S.R. Nagel, *Science* **255**, 1523 (1992).
[5] H.M. Jaeger, S.R. Nagel, and R.P. Behringer, *Rev. Mod. Phys* **68**, 1259 (1996).
[6] M. Nicodemi and A. Coniglio, *Phys. Rev. Lett.* **82**, 916 (1999).
[7] A. Barrat, V. Loreto, *J. Phys. A.* **33**, 4401 (2000)
[8] C. Josserand, A.V. Tkachenko, D.M. Mueth and H.M. Jaeger, *Phys. Rev. Lett.* **85**, 3632 (2000).
[9] A. Barrat, V. Loreto, *Europhys. Lett.* **53**, 297 (2001).
[10] J. B. Knight, C. G. Fandrich, C. N. Lau, H. M. Jaeger, and S. R. Nagel, *Phys. Rev. E* **51**, 3957 (1995).
[11] S.F. Edwards, in: *Granular Matter: An Interdisciplinary Approach*, A. Mehta, Ed. (Springer-Verlag, New York, 1994), and references therein.
[12] S.F. Edwards, in: *Disorder in Condensed Matter Physics*, Blackman, J.A. and Taguena, J., Eds., (Oxford University Press, Oxford, 1991).
[13] A. Mehta, R.J. Needs, S. Dattagupta, *J. Stat. Phys.* **68**, 1131 (1992).
[14] R. Monasson, O. Pouliquen, *Physica A* **236**, 395 (1997).
[15] It is important to stress how the actual definition of blocked configurations or blocked particles depends crucially on the system or model one is considering. For instance in systems subject to gravity one could identify a blocked configuration as a configuration stable under the effect of the gravity. More in general one has to identify the mechanisms responsible for the frustration and define the blocked configurations in a consistent way. There has been a recent argument [16] which suggests that an im-

portant role for the dynamics is played by the ability or lack of rolling of one particle relative to neighbours in contact, i.e. the friction.
[16] R.C. Ball and R. Blumenfeld, cond-mat/0008127.
[17] See, for example Chapter 7 of: L.C.E. Struik, *Physical Ageing in Amorphous Polymers and Other materials*, (Elsevier, Houston, 1978).
[18] W. Kob, H.C. Andersen, *Phys. Rev. E* **48**, 4364 (1993).
[19] E. Caglioti, V. Loreto, H.J. Herrmann and M. Nicodemi, *Phys. Rev. Lett.* **79**, 1575 (1997).
[20] T.R. Kirkpatrick, D. Thirumalai, *Phys. Rev. B* **36**, 5388 (1987).
[21] T.R. Kirkpatrick, P.G. Wolynes, *Phys. Rev. A* **35**, 3072 (1987).
[22] J.-P. Bouchaud, L.F. Cugliandolo, J. Kurchan and M. Mézard, in *Spin-glasses and random fields*, A. P. Young, Ed. (World Scientific, Singapore, 1997).
[23] L.F. Cugliandolo, J. Kurchan, L. Peliti, *Phys. Rev. E* **55**, 3898 (1997).
[24] R. Monasson, *Phys. Rev. Lett.* **75**, 2847 (1995).
[25] J. Kurchan, in *Jamming and Rheology: Constrained Dynamics on Microscopic and Macroscopic Scales* (1997), http://www.itp.ucsb.edu/online/jamming2/, and Edwards, S.F., Liu, A. and Nagel, S.R. Eds., to be published, cond-mat 9812347.
[26] Th.M. Nieuwenhuizen, *Phys. Rev. E* **61**, 267 (2000).
[27] S. Franz, M.A. Virasoro, *J. Phys. A* **33**, 891 (2000).
[28] A. Crisanti, F. Ritort, *Europhys. Lett.* **52**, 640 (2000).
[29] G. Biroli and J. Kurchan, *Phys. Rev.* **E**, to be published (cond-mat/0005499).
[30] J. Kurchan, *J. Phys. Condensed Matter*, **12**, 6611 (2000).
[31] E. Caglioti, A. Coniglio, H.J. Herrmann, V. Loreto and M. Nicodemi, *Physica A* **265**, 311 (1999).
[32] E. Ben-Naim, J.B. Knight and E.R. Nowak, *Physica D* **123**, 380 (1998); P.L Krapivsky and E. Ben-Naim, *J. of Chem. Phys.* **100**, 6778 (1994).
[33] T. Boutreux and P.G. de Gennes, in *Powders and Grains 97*, edited by R. Behringer and J. Jenkins (A.A. Balkema, Rotterdam), pp.439.
[34] for a general introduction see: D.W. Jordan and P. Smith, *Nonlinear Ordinary Differential Equations*, Oxford, England, Clarendon Press (1977).
[35] The functional F is concave because is given by the sum of a linear term, which is irrelevant for the concavity, and of a concave term $S(\rho_k)$. Since the sum of concave functions is concave one gets the desired result. On the other hand one can look at the hessian matrix and realize that it is diagonal with all diagonal terms given by $\partial^2 F/\partial\rho_k^2 = \partial^2 S/\partial\rho_k^2 \geq 0 \ \forall k$.
[36] E. Clement and J. Rajchenbach, *Europhys. Lett.* **16**, 133 (1991).
[37] E. Caglioti, A. Coniglio, H.J. Herrmann, V. Loreto and M. Nicodemi, *Europhys. Lett.* **43**, 591 (1998).
[38] For a review, see: W. Götze, in 'Liquids, freezing and glass transition', J.P. Hansen, D. Levesque, J. Zinn-Justin Editors, Les Houches (1989) (North Holland).
[39] J. Kurchan, L. Peliti, M. Sellitto, *Europhys. Lett.* **39**, 365 (1997).
[40] M. Sellitto, *Euro. J. Phys. B* **4**, 135 (1998).
[41] M. Sellitto, J.J. Arenzon, *Phys. Rev. E* **62** 7793 (2000).
[42] M. Piccioni, V. Loreto and S. Roux, *Phys. Rev. E* **61**, 2813 (1999).
[43] V. Colizza, A. Barrat and V. Loreto, in preparation (2001).
[44] E. Ott, *Chaos in Dynamical Systems* (Cambridge University Press, Cambridge 1993).